AIP | Journal of Applied Physics

Characteristic free volume change of bulk metallic glasses

Qiang Hu, Xie-Rong Zeng, and M. W. Fu

Citation: J. Appl. Phys. **111**, 083523 (2012); doi: 10.1063/1.4704688
View online: http://dx.doi.org/10.1063/1.4704688
View Table of Contents: http://jap.aip.org/resource/1/JAPIAU/v111/i8
Published by the American Institute of Physics.

Characteristic free volume change of bulk metallic glasses

Qiang Hu,[1] Xie-Rong Zeng,[2,3,a)] and M. W. Fu[4]
[1]*School of Materials Science and Engineering, Northwestern Polytechnical University, Xi'an, Shaanxi 710072, People's Republic of China*
[2]*College of Materials Science and Engineering, Shenzhen University, Shenzhen 518060, People's Republic of China*
[3]*Shenzhen Key Laboratory of Special Functional Materials, Shenzhen 518060, People's Republic of China*
[4]*Department of Mechanical Engineering, The Hong Kong Polytechnic University, Hong Kong, People's Republic of China*

(Received 17 December 2011; accepted 16 March 2012; published online 23 April 2012)

The free volume change $\Delta V_f(T)$ of bulk metallic glasses (BMGs) relative to a hypothesized amorphous reference state was measured using the thermal dilatation method. The characteristic free volume change, i.e., the free volume released in structural relaxation $\Delta V_{f\text{-}sr}$, was identified quantitatively from the $\Delta V_f(T)$ curve. For a Fe-based BMG, it was found that $\Delta V_{f\text{-}sr}$ increases with decreases in the sample diameter and heating rate. $\Delta V_{f\text{-}sr}$ measured under the same sample diameter and heating rate conditions allowed the convenient comparison of different BMGs. The comparison revealed that the glass-forming ability (GFA) enhancement of each of two Pd-, Mg-, Cu-, Zr-, Ti-, and Fe-based BMGs can be sensitively reflected in the decrease in $\Delta V_{f\text{-}sr}$ and the narrowing of the difference between the peak temperature of the thermal expansion coefficient and the end temperature of the glass transition process. In addition, for these twelve typical BMGs, there is a good linear relationship between $\Delta V_{f\text{-}sr}$ and $\mathrm{Log}D_c^2$ or $\mathrm{Log}D_c$, where D_c is the critical diameter. $\Delta V_{f\text{-}sr}$ is thus sensitive to and has a close correlation with GFA. Furthermore, the $\Delta V_{f\text{-}sr}$ measurement results are in good agreement with the free volume change measured with the specific heat capacity, room temperature density, and positron annihilation lifetime methods. In the study of the relationship between the structure and properties of BMGs, $\Delta V_{f\text{-}sr}$ thus plays an important role given its comparability and convenience. © *2012 American Institute of Physics*. [http://dx.doi.org/10.1063/1.4704688]

I. INTRODUCTION

Free volume is a widely used concept related to the structure and properties of bulk metallic glasses (BMGs) such as glass-forming ability (GFA),[1,2] mechanical properties,[3] inelastic deformation,[4] and the Invar effect.[5] The absolute value of the free volume $V_f(T)$ contained in BMGs at a given temperature is, however, difficult to measure because it is impossible to obtain a reference amorphous state without any free volume in an experiment.[6] Therefore, rather than the absolute free volume value $V_f(T)$, the free volume change $\Delta V_f(T)$ relative to the crystalline or relaxed amorphous state is usually measured on the basis of the variation in some other physical parameters with a change in temperature. However, a number of difficulties remain in the measurement of $\Delta V_f(T)$. For example, Beukel *et al.*[7–11] showed that the specific heat capacity ΔC_p is proportional to the temperature derivative of free volume, although ΔC_p by itself cannot be employed to compare the $\Delta V_f(T)$ of different compositions for the undetermined composition-dependent proportional coefficient. A similar restriction is imposed on the positron lifetime τ, which is sensitive to differences in electron density and is prolonged in vacancies.[12–15] Room temperature density ρ (Refs. 8, 15–17) is a convenient, but not real-time, parameter. It can be employed to determine ΔV_f after heating but not during the heating process, particularly in the glass transition process. The change in the maximum wave-vector $[(Q_{max}(T^{room}))/Q_{max}(T)]^3$, which is measured by real-time high-energy synchrotron radiation x-ray diffraction (XRD), is equal to the volume change $[(V(T))/V(T^{room})]$. The $\Delta V_f(T)$ between the as-cast and relaxed states of BMGs can be quantified *in situ* as the $[(Q_{max}(T^{room}))/Q_{max}(T)]^3$ difference between the heating and reheating processes at glass transition temperature T_g, according to the work carried out by Yavari *et al.*[18–21] However, this method does not clearly articulate how the free volume changes in the glass transition process because both the as-cast and reference relaxed amorphous states undergo glass transition. The development of a $\Delta V_f(T)$ measurement that is real-time and allows convenient comparisons among different compositions thus remains a challenge.

Regardless of the complexity of the original definition of free volume, as elaborated upon by Cohen and Turnbull,[22–25] the free volume of BMGs is actually a part of their volume and changes with temperature. The volume change of isotropic BMGs during the heating process is three times their dimension change.[9,11,12,26–28] It is thus possible to measure the free volume change using the thermal dilatation (DIL) test, and a DIL test-based method for measuring $\Delta V_f(T)$ was recently developed.[1] The characteristic free volume change, i.e., the free volume released in structural relaxation $\Delta V_{f\text{-}sr}$, is identified quantitatively from the $\Delta V_f(T)$ curve. For a series of Fe-(Er)-Cr-Mo-C-B BMGs, $\Delta V_{f\text{-}sr}$ is sensitive to and closely correlated with GFA.[1,2] This paper

a)Electronic mail: zengxier@szu.edu.cn.

presents a more detailed description of this measurement method. The sample diameter and heating rate effects on the $\Delta V_{f\text{-}sr}$ of Fe-based BMGs are investigated and analyzed. A systematic investigation of the correlation between the $\Delta V_{f\text{-}sr}$ and GFA of 12 typical BMGs with 6 base metals, and that between the peak temperature of thermal expansion coefficient $T_{\alpha\text{-}p}$ and the ending temperature of the glass transition process $T_{g\text{-}end}$, is also conducted. Finally, the validity of $\Delta V_{f\text{-}sr}$ for measurement purposes is confirmed via comparison between $\Delta V_{f\text{-}sr}$ and the free volume change measured with the specific heat capacity, room temperature density, and positron annihilation lifetime methods.

II. EXPERIMENT

$Fe_{41}Co_7Cr_{15}Mo_{14}C_{15}B_6Y_2$ (Ref. 36) BMG rods with diameters (D) of 1.0, 2.0, 3.0, and 5.0 mm and Pd- (Refs. 29 and 30), Mg- (Refs. 31 and 32), Cu- (Ref. 33), Zr- (Ref. 34), Ti- (Ref. 35), and Fe- (Ref. 37) based BMGs rods with a D of 2.0 mm were prepared using copper-mold casting (RAPID QUENCH MACHINE SYSTEM VF-RQT50, MAKABE). The original length of the as-cast rods was 50 mm. The amorphous states of the as-cast samples were confirmed by XRD (D8 ADVANCE, BRUKER) and differential scanning calorimetry (DSC; SETSYS Evolution 1750, SETARAM). Rod samples with a length L_0 of 25.0±0.1 mm were cut from the middle of the as-cast rods, with their two ends carefully polished to ensure parallelity. DIL tests were performed in a thermal dilatometer (DIL 402 C, NETZSCH) with a resolution of 1.25 nm. The equipment was calibrated with an alumina standard sample at heating rates of 2.5, 5, 10, and 20 K/min, and flushed with a high-purity argon flow at 100 ml/min for 10 min before the test and at 50 ml/min during it. The applied load was 0.3 N. Accuracy was ensured during the measurement process by the very low-thermal expansion of the Invar measurement system at a constant temperature ($20.0 \pm 0.1\,^{\circ}C$) maintained by the circulating coolant liquid.[38] Data on linear thermal expansion $\Delta L(T)/L_0$ and the linear thermal expansion coefficient $\alpha_L(T)$ ($\alpha_L(T) = 1/L(T) \times dL(T)/dT$) were recorded in the tests.

III. RESULTS AND DISCUSSION

A. Definitions of $\Delta V_{f\text{-}sr}$ and $\Delta V_{f\text{-}gt}$

Figure 1(a) is a sketch of the typical absolute free volume $V_f(T)$ and the equilibrium free volume line, which is valid only in a narrow region around T_g (Ref. 7). The initial free volume V_{f0} does not change until the onset temperature of structural relaxation $T_{sr\text{-}on}$ is reached. At $T_{sr\text{-}on}$, the free volume begins to be released due to atomic mobility.[39] Above $T_{sr\text{-}on}$, $V_f(T)$ decreases continuously until it intersects the equilibrium line at the point of ($T_{sr\text{-}end}$, $V_{f\text{-}re}$). $T_{sr\text{-}end}$ is both the ending temperature of structural relaxation and the onset temperature of the glass transition. $V_{f\text{-}re}$ is the residual free volume contained in the amorphous solid after structural relaxation and before glass transition. To return to the equilibrium state, $V_f(T)$ must increase above $T_{sr\text{-}end}$, finally coinciding with the equilibrium line at the point of ($T_{g\text{-}end}$, $V_{f\text{-}scl}$). $T_{g\text{-}end}$ is both the ending temperature of the glass transition and the onset temperature of the super-cooled liquid region. At $T_{g\text{-}end}$, the glassy solid is completely transformed into a super-cooled liquid with a free volume of $V_{f\text{-}scl}$. The glass transition from point ($T_{sr\text{-}end}$, $V_{f\text{-}re}$) to point ($T_{g\text{-}end}$, $V_{f\text{-}scl}$) is a free volume generation process, which occurs only with continuous heating.[39] As shown in Fig. 1, $\Delta V_{f\text{-}sr}$ and $\Delta V_{f\text{-}gt}$ are defined as quantifying the characteristic free volume changes in the structural relaxation and glass transition processes, respectively. The temperature intervals of these two processes are ΔT_{sr} and ΔT_{gt}. They are formulated as follows:

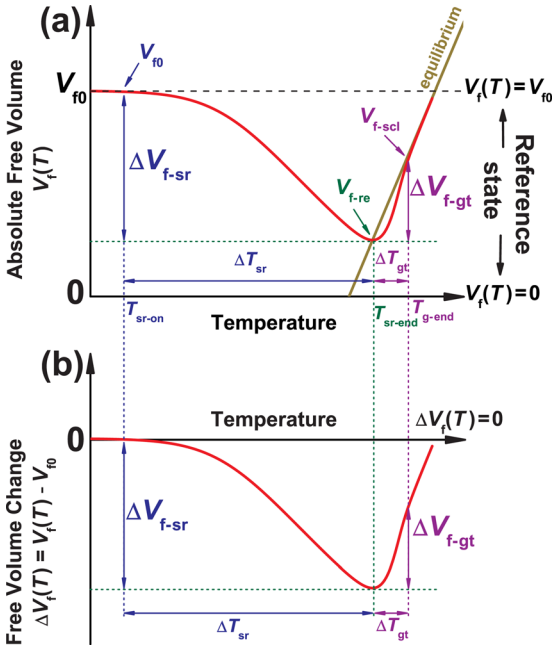

FIG. 1. Sketch of (a) equilibrium free volume line and absolute free volume $V_f(T)$ relative to the reference state $V_f(T) = 0$ and (b) free volume change $\Delta V_f(T)$ relative to the reference state $V_f(T) = V_{f0}$.

$$\Delta V_{f\text{-}sr} = V_{f0} - V_{f\text{-}re}, \quad \Delta T_{sr} = T_{sr\text{-}end} - T_{sr\text{-}on}, \tag{1}$$

$$\Delta V_{f\text{-}gt} = V_{f\text{-}scl} - V_{f\text{-}re}, \quad \Delta T_{gt} = T_{g\text{-}end} - T_{sr\text{-}end}. \tag{2}$$

The reference state of Fig. 1(a) is the amorphous state with absolute zero free volume at any temperature, i.e., $V_f(T) = 0$. However, it is impossible to obtain an amorphous state without any free volume in the temperature region around T_g even after a very long period of annealing below T_g (Refs. 6 and 40). Hence, in practice, the alternative crystalline state is adopted in both the specific heat capacity and positron lifetime methods,[7,8,14] although the packing density of this state differs from that of the amorphous state. In addition, the alternative relaxed amorphous state is employed in the room temperature density and maximum wave-vector methods.[8,15–21] The free volume generated in the glass transition process of the relaxed amorphous state, however, is greater than that of the as-cast amorphous state.

The other alternative reference state is the amorphous state with a constant free volume V_{f0} at any temperature, i.e., the straight dashed line $V_f(T) = V_{f0}$ shown in Fig. 1(a). The free volume change with temperature relative to this reference state is $\Delta V_f(T) = V_f(T) - V_{f0}$, as shown in Fig. 1(b). Although the absolute values of V_{f0}, $V_{f\text{-}re}$, and $V_{f\text{-}scl}$ remain unknown, $\Delta V_{f\text{-}sr}$,

$\Delta V_{f\text{-}gt}$, ΔV_{sr}, and ΔT_{gt} can be determined from the $\Delta V_f(T)$ curve in Fig. 1(b). The key point to measuring the two characteristic free volume changes is thus to find a reference amorphous state with a constant ΔV_{f0} at any temperature. Certainly, this kind of reference amorphous state cannot be obtained by experimentation, but Sec. III B articulates a way to hypothesize it.

B. Quantification of $\Delta V_{f\text{-}sr}$ from the $\Delta V_f(T)$ curve measured using the DIL method

It can be seen from Fig. 2(a) that it is difficult to observe the free volume change from the experimental DIL trace directly because it is concealed by the comparatively larger linear thermal expansion.[11,18–21,26–28,41] Fig. 2(b) shows the similarity of the DSC traces and the thermal expansion coefficient $\alpha_L(T)$ trace above the onset crystallization temperature $T_{x\text{-}on}$. In the crystallization process, the atomic rearrangement from disorder to order results in the simultaneous energy release shown in the DSC trace and the volume shrinkage shown in the $\alpha_L(T)$ trace. Fig. 2(c) shows a peak in the $\alpha_L(T)$ trace around the glass transition point. On the one hand, $\alpha_L(T)$ obviously increases due to the free volume generation in the glass transition process. On the other hand, the amorphous solid is gradually transformed into the supercooled liquid in this process. The increase in liquid content results in a decrease in viscosity. Under the compressive load of 0.3 N exerted by the DIL instrument, $\alpha_L(T)$ drops dramatically, and the softening begins at the peak temperature of $T_{\alpha\text{-}p}$. $T_{\alpha\text{-}p}$ depends on how fast the viscosity decreases with temperature in the glass transition process and how great the compressive stress is. In other words, $T_{\alpha\text{-}p}$ is determined by the composition and diameter of the sample. For the $Fe_{41}Co_7Cr_{15}Mo_{14}C_{15}B_6Y_2$ BMG rod with a diameter of 3.0 mm, $T_{\alpha\text{-}p}$ (867.4±1.6 K) is slightly lower than $T_{g\text{-}end}$ (868.1±2.3 K) in the DSC trace, as shown in Fig. 2(c). The difference between $T_{\alpha\text{-}p}$ and $T_{g\text{-}end}$ will be discussed in Secs. III C 3 and III D 1.

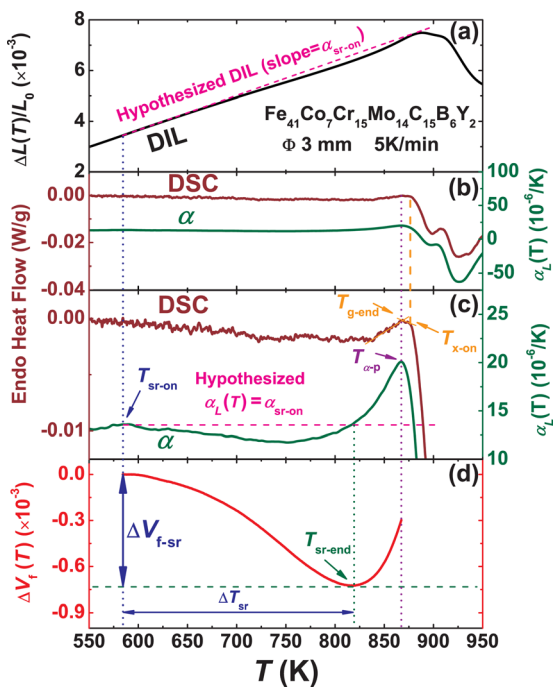

FIG. 2. (a) Experimental and hypothesized DIL traces. DSC and $\alpha_L(T)$ traces with (b) large- and (c) small-scale vertical coordinates. (d) The corresponding $\Delta V_f(T)$ curve.

In addition, with the free volume release shown in Fig. 2(c), $\alpha_L(T)$ decreases steadily above $T_{sr\text{-}on}$. The small free volume change in the low-temperature region below $T_{sr\text{-}on}$ that is due to the variation in the chemical short range order[7,26] is not considered in this research. This research focuses only on the obvious free volume change in the high-temperature region above $T_{sr\text{-}on}$, which is related primarily to the variation in the topological short range order.[7] $T_{sr\text{-}on}$ thus corresponds to the onset temperature of the main structural relaxation. At $T_{sr\text{-}on}$, the free volume contained in the sample is assumed to be the initial free volume V_{f0}. Above $T_{sr\text{-}on}$, if the free volume does not change with temperature, then V_{f0} remains the same, $\alpha_L(T)$ has a constant value $\alpha_{sr\text{-}on}$, as shown in the hypothesized $\alpha_L(T)$ trace in Fig. 2(c), and the sample expands linearly at constant slope $\alpha_{sr\text{-}on}$ as shown in the hypothesized DIL trace in Fig. 2(a). The hypothesized DIL trace is thus the thermal expansion of the reference amorphous state with a constant V_{f0}, which is exactly the reference amorphous state depicted in Fig. 1. Consequently, the free volume change ΔV_f relative to this hypothesized reference amorphous state as a function of temperature, i.e., from $T_{sr\text{-}on}$ to $T_{\alpha\text{-}p}$, can be calculated by integrating the difference between the experimental $\alpha_L(T)$ trace and hypothesized $\alpha_L(T)$ trace or, more simply, by subtracting the hypothesized DIL trace $\Delta L'(T)/L_0$ from the experimental trace $\Delta L(T)/L_0$, as follows:

$$\Delta V_f(T) = 3 \times \int_{T_{sr\text{-}on}}^{T} (\alpha_L(T) - \alpha_{sr\text{-}on})dT = 3 \times \left(\frac{\Delta L(T)}{L_0} - \frac{\Delta L'(T)}{L_0}\right) (T_{\alpha\text{-}p} \geq T \geq T_{sr\text{-}on}), \quad (3)$$

where the hypothesized DIL trace $\Delta L'(T)/L_0$ is

$$\frac{\Delta L'(T)}{L_0} = \frac{\Delta L(T_{sr\text{-}on})}{L_0} + \alpha_{sr\text{-}on} \times (T - T_{sr\text{-}on}) \quad (T \geq T_{sr\text{-}on}). \quad (4)$$

The premise of Eq. (3) is $\Delta V(T)/V_0 = \int \alpha_V(T)dT = 3 \times \int \alpha_L(T)dT = 3 \times \Delta L(T)/L_0$, where the volume thermal expansion coefficient $\alpha_V(T)$ is $\alpha_V(T) = 1/V(T) \times dV(T)/dT$. This linear relation premise, however, is invalid above $T_{\alpha\text{-}p}$ because the sample begins to soften at $T_{\alpha\text{-}p}$.[28] Therefore, the free volume generation above $T_{\alpha\text{-}p}$ could not be observed in the DIL test. Although the $\Delta V_f(T)$ measured with the DIL method describes only the free volume change from $T_{sr\text{-}on}$ to $T_{\alpha\text{-}p}$, the change trend in Fig. 2(d) is in good agreement with that of the sketch in Fig. 1(b). As shown in Fig. 2(d), the lowest temperature $T_{sr\text{-}end}$, which is also the intersection temperature between the experimental $\alpha_L(T)$ and hypothesized $\alpha_L(T)$ traces, corresponds to the ending temperature of structural relaxation and the beginning temperature of the glass transition. Both the temperature interval of the structural relaxation process ΔT_{sr} and the first characteristic free volume change

$\Delta V_{f\text{-}sr}$ can be quantified as in Fig. 2(d). The quantification of $\Delta V_{f\text{-}sr}$ and ΔT_{sr} in Fig. 2(d) is the same as that in Fig. 1(b). The second characteristic free volume change $\Delta V_{f\text{-}gt}$, in contrast, cannot be accurately quantified by the $\Delta V_f(T)$ curve in Fig. 2(d), and its investigation is thus omitted from this research. The detailed reasons for this omission are provided in Secs. III C 3 and III D 1.

The composition-dependent proportional coefficient is required to measure the free volume change using the specific heat capacity method,[8] although no additional parameters are needed to determine the $\Delta V_f(T)$ with the DIL method, as previously noted. $\Delta V_f(T)$ is thus convenient for comparing the measurement results of different BMGs. To render this comparison more accurate, it is necessary to investigate how factors other than BMG composition affect $\Delta V_f(T)$. The most important experimental parameters in the DIL test are the sample diameter D and heating rate R_h. Their effects are discussed in Sec. III C.

C. Sample diameter and heating rate effects on $\Delta V_f(T)$

Figure 3, Table I, and Fig. 4 present the measurement results for different D and R_h. In each group of tests, one parameter was changed and the other kept the same. As shown in Table I, $\alpha_{sr\text{-}on}$ undergoes a slight increase and $T_{sr\text{-}on}$ changes little with a change in D and R_h. For the $Fe_{41}Co_7Cr_{15}Mo_{14}C_{15}B_6Y_2$ BMG, the hypothesized DIL trace, which is determined by $\alpha_{sr\text{-}on}$ and $T_{sr\text{-}on}$ based on Eq. (4) and deemed to be the thermal expansion of the hypothesized reference amorphous state, shows little variation across tests. Hence, the $\Delta V_f(T)$ in different conditions is dependent primarily on the experimental thermal expansion above $T_{sr\text{-}on}$. Five tests were carried out for the Φ 3.0 mm sample measured at 5 K/min and two tests for the other conditions. The repeatability errors of $\Delta V_{f\text{-}sr}$ were 0.03-0.04 $\times 10^{-3}$ for most of the tests, but were 0.05-0.06 $\times 10^{-3}$ for the test on (Φ 5.0 mm, 5 K/min) and 0.08-0.1 $\times 10^{-3}$ for that on (Φ 3.0 mm, 20 K/min). Different from the 20 ~ 30 mg sample used in the DSC test, the mass of the Fe-based BMG rod samples used in the DIL tests ranged from 0.2 ~ 3.6 g, depending on the D. Furthermore, different from the non-contact dilatometer developed by Ye *et al.*, which is able to support a high R_h of 80 K/min,[12] the thermo-mechanical dilatometer used in the current study (DIL 402 C, Netzsch) becomes unstable at any R_h larger than 30 K/min. A large sample mass and higher heating rate would affect the uniformity of the sample temperature and cause a large degree of error. However, when considering the 0.5 $\times 10^{-3}$ order of the characteristic free volume changes, the error is acceptable.

1. Sample diameter effect

Figure 3(a1) shows the divergence between the experimental and hypothesized DIL traces to increase with a decrease in D. It can be seen from Fig. 3(a3) that the smaller samples have a smaller $\alpha_L(T)$ value above $T_{sr\text{-}on}$. The structural difference between the samples with a different D lies primarily in their different initial V_{f0}. The initial V_{f0} contained in the amorphous solid is closely related to the cooling process of liquid metal. A faster cooling rate allows a greater free volume of liquid to be frozen into the amorphous solid.[39,42]

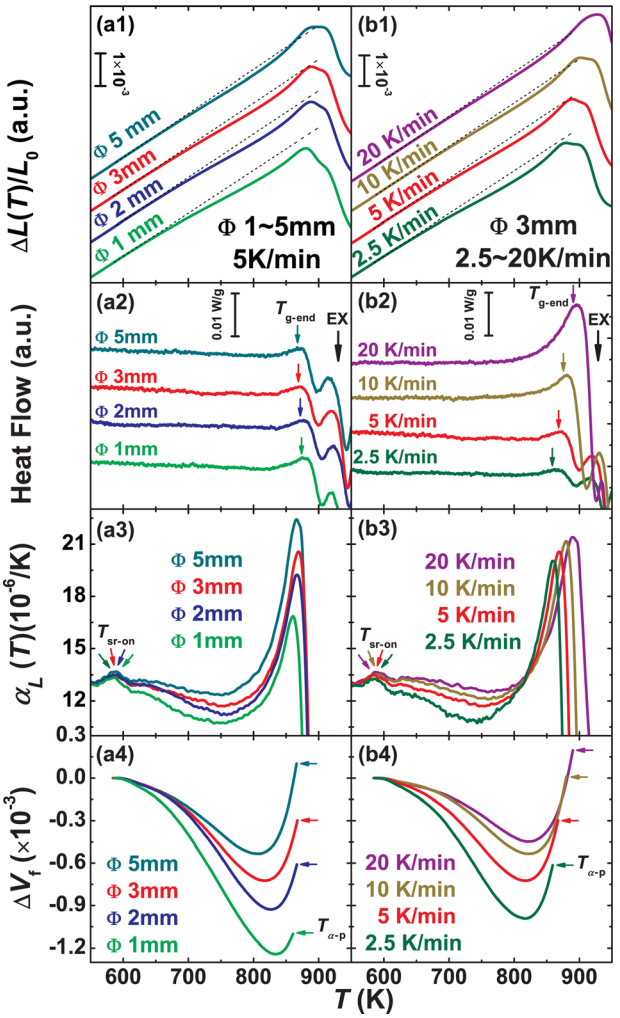

FIG. 3. (a1, b1) Experimental and hypothesized DIL traces, (a2, b2) DSC traces, (a3, b3) $\alpha_L(T)$ traces, and (a4, b4) $\Delta V_f(T)$ curves of $Fe_{41}Co_7Cr_{15}Mo_{14}C_{15}B_6Y_2$ BMGs with different sample diameters and heating rates. The hypothesized $\alpha_L(T)$ traces are not plotted for a clearer display.

According to the approximate inverse square relation between the cooling rate and sample dimensions proposed by Johnson *et al.*,[43] the cooling rate employed in fabricating the samples with a D of 1.0, 2.0, 3.0, and 5.0 mm is estimated to be 4.0 $\times 10^3$ K/s, 1.0 $\times 10^3$ K/s, 4.4 $\times 10^2$ K/s, and 1.6 $\times 10^2$ K/s, respectively. The absolute value of V_{f0} cannot be determined on the basis of the $\Delta V_f(T)$ curves, despite the smaller samples prepared with a faster cooling rate having a larger

TABLE I. $T_{sr\text{-}on}$ and $\alpha_{sr\text{-}on}$ of $Fe_{41}Co_7Cr_{15}Mo_{14}C_{15}B_6Y_2$ BMG rods under different conditions of sample diameter (D) and heating rate (R_h).

D (mm)	R_h (K/min)	$\alpha_{sr\text{-}on}$ (10^{-6}/K)	$T_{sr\text{-}on}$ (K)
1.0	5.0	13.35 ± 0.11	586.4 ± 1.1
2.0		13.49 ± 0.06	589.9 ± 1.4
3.0		13.50 ± 0.04	587.2 ± 0.9
5.0		13.69 ± 0.06	588.8 ± 2.1
3.0	2.5	13.28 ± 0.07	588.9 ± 1.1
	5.0	13.50 ± 0.04	587.2 ± 0.9
	10.0	13.53 ± 0.10	587.8 ± 1.7
	20.0	13.66 ± 0.16	586.7 ± 2.6

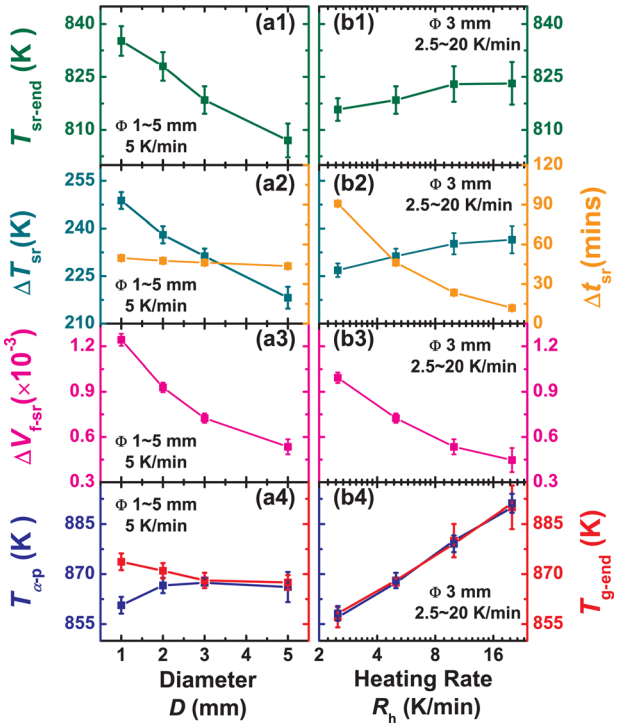

FIG. 4. The effects of sample diameter and heating rate on (a1, b1) $T_{sr\text{-}end}$, (a2, b2) ΔT_{sr} and Δt_{sr}, (a3, b3) $\Delta V_{f\text{-}sr}$, and (a4, b4) $T_{\alpha\text{-}p}$ and $T_{g\text{-}end}$.

initial V_{f0} (Ref. 42). In addition, the absolute value of the residual $V_{f\text{-}re}$ remains unknown, although Fig. 4(a1) shows the smaller diameter sample to have a higher $T_{sr\text{-}end}$ and thus a larger residual $V_{f\text{-}re}$. Furthermore, Fig. 4(a3) shows the smaller sample also to have a larger $\Delta V_{f\text{-}sr}$. After structural relaxation, a part of the initial V_{f0} is released as $\Delta V_{f\text{-}sr}$, and the residual component is $V_{f\text{-}re}$. Based on Eq. (1), the foregoing process can be further quantified as

$$\Delta V_{f\text{-}sr} = V_{f0} \times \lambda \tag{5}$$

$$V_{f\text{-}re} = V_{f0} - \Delta V_{f\text{-}sr} = V_{f0} \times (1 - \lambda). \tag{6}$$

If the ratios λ of the four samples differ greatly, then it is impossible for V_{f0}, $\Delta V_{f\text{-}sr}$, and $V_{f\text{-}re}$ to all increase at the same time with a decrease in D, which means either that V_{f0} and $\Delta V_{f\text{-}sr}$ increase while $V_{f\text{-}re}$ decreases or that V_{f0} and $V_{f\text{-}re}$ increase while $\Delta V_{f\text{-}sr}$ decreases. Hence, it is reasonable to deduce that the four samples with different D have similar λ. Only under this condition can V_{f0}, $\Delta V_{f\text{-}sr}$ and $V_{f\text{-}re}$ increase at the same time with a decrease in D. This ratio λ represents the degree of structural relaxation, which is dependent primarily on how long such relaxation is sustained. As shown in Fig. 4(a2), the time interval of structural relaxation Δt_{sr} changes little with D, which confirms the similarity of λ in the different samples tested with the same R_h. In addition, with the same R_h, the smaller sample with a larger V_{f0} requires a wider temperature interval ΔT_{sr} to release a larger $\Delta V_{f\text{-}sr}$, as shown in Fig. 4(a2).

2. Heating rate effect

Figure 3(b1) shows the experimental DIL traces measured with a faster R_h to be closer to the hypothesized DIL traces. It can be seen from Fig. 3(b2) that $\alpha_L(T)$ decreases less during structural relaxation and increases more during the glass transition in the test with a faster R_h. The samples with the same D had the same initial V_{f0} and compressive stress applied to them. In the test with a faster R_h, $T_{sr\text{-}end}$ shifted to a higher temperature, as shown in Fig. 4(b1), and the residual $V_{f\text{-}re}$ consequently grew larger. The ratio λ in Eq. (5) thus decreases with a faster R_h. The temperature interval ΔT_{sr} increases slightly, whereas the time interval Δt_{sr} undergoes an obvious decrease with a faster R_h, as shown in Fig. 4(b2), which also indicates a less insufficient degree of structural relaxation and a smaller ratio λ with a faster R_h. Whether based on Eq. (1) or (5), a smaller $\Delta V_{f\text{-}sr}$ will be obtained in a test with a faster R_h, as shown in Fig. 4(b3).

3. Difference between $T_{\alpha\text{-}p}$ and $T_{g\text{-}end}$

Figures 4(a4) and 4(b4) show the $T_{\alpha\text{-}p}$ determined by the DIL tests and $T_{g\text{-}end}$ determined by the DSC tests under different conditions of D and R_h. The increase in $T_{g\text{-}end}$ with a faster R_h shown in Fig. 4(b4) is a natural characteristic of glass.[44–46] Among the samples with a D of 3 mm tested with different R_h, $T_{\alpha\text{-}p}$ has good agreement with $T_{g\text{-}end}$ with an acceptable degree of experimental error. Fig. 4(a4) shows that the smaller sample prepared at a faster cooling rate has a slightly higher $T_{g\text{-}end}$. This weak positive dependence of $T_{g\text{-}end}$ on the fabrication cooling rate is another natural characteristic of glass.[44] The $T_{\alpha\text{-}p}$ of the samples with a D of 1.0 and 2.0 mm, however, is obviously lower than the $T_{g\text{-}end}$. The compressive stress $(0.3/(\pi(D/2)^2))$ applied to the samples with a D of 1.0, 2.0, 3.0, and 5.0 mm was 382, 95, 42, and 15 KPa, respectively. Compared to the strength of the $Fe_{41}Co_7Cr_{15}Mo_{14}C_{15}B_6Y_2$ BMG with 3500 MPa,[36] the compressive stress exerted by the instrument was too small to affect the thermal expansion of the solid sample. Therefore, the measurement results for $\Delta V_f(T)$ below $T_{sr\text{-}end}$ and $\Delta V_{f\text{-}sr}$ are reliable. Above $T_{sr\text{-}end}$, a glassy solid is gradually transformed into a super-cooled liquid via the glass transition process. In this transition process, the sample structure consisted of a glassy solid and a super-cooled liquid, a type of structure that is a non-Newtonian fluid whose viscosity depends on the compressive stress.[28] Before the glass transition had finished, i.e., when some of the solids had not yet been transformed into liquids, the viscosities of the samples with diameters of 1.0 and 2.0 mm to which a relatively large compressive stress had been applied were sufficiently low to facilitate the softening occurring at $T_{\alpha\text{-}p}$. For the small samples, the $T_{\alpha\text{-}p}$ was thus obviously lower than the $T_{g\text{-}end}$, which constitutes the major difference between the observed glass transition behavior in the DIL and DSC tests. Furthermore, in addition to D, BMG composition also affects the $T_{\alpha\text{-}p}$, which will be discussed in Sec. III D 1. Hence, it does not make sense to use the DIL method to measure incomplete free volume generation.

In general, both D and R_h were found to have clear effects on $\Delta V_f(T)$. The DIL method is unable to measure the entire free volume generation in the glass transition process accurately because of the sample softening effect. $\Delta V_{f\text{-}sr}$, in contrast, describes the free volume change in an amorphous solid, and is thus independent of compressive stress. For the

same D and R_h, $\Delta V_{f\text{-}sr}$, as measured using the DIL method, can be reliably employed to make comparisons among different BMGs. Such comparison allows the correlation between the structure and properties of different BMGs, including GFA, to be investigated quantitatively.

D. Study of GFA by ($T_{\alpha\text{-}p}$-$T_{g\text{-}end}$) and $\Delta V_{f\text{-}sr}$

GFA is one of the most important issues in BMG research. A number of physical parameters have been found to be correlated with GFA, such as the fragility of liquid metal,[47–49] the viscosity at the melting point,[50] the volumetric change from glass transition to melting,[51] and the density change upon crystallization.[2] The free volume concept is often involved in these findings. To date, however, there has been no systematic investigation of the correlation between free volume and GFA, due to the lack of a free volume measurement method that provides comparable results for different compositions. Although the DIL method is unable to determine the absolute value of the initial free volume V_{f0} contained in as-cast samples, a comparison of $\Delta V_{f\text{-}sr}$, which reflects the amorphous solid structural features of different BMGs, is useful for investigating GFA. As studied in Sec. III C, the $\Delta V_{f\text{-}sr}$ of the sample with a smaller D measured at a slower R_h had a larger value, which allows more effective comparisons among different BMGs. The smallest critical diameter (D_c) among the 12 typical Pd-, Mg-, Cu-, Zr-, Ti-, and Fe-BMGs was 2.5 mm for the $Ti_{42.5}Zr_{2.5}Hf_5Cu_{42.5}Ni_{7.5}$ BMG (Ref. 35). Therefore, samples with a D of 2.0 mm were used in the DIL tests. An R_h of 5 K/min was adopted to save time. The tests were performed two to three times, and the results are shown in Fig. 5 and Table II. The $\Delta V_{f\text{-}sr}$ errors are $0.03\text{-}0.06 \times 10^{-3}$ for most compositions, except for $0.10\text{-}0.11 \times 10^{-3}$ for the two Mg-based BMGs. It is difficult to control the volatilization amount of Mg when preparing Mg-based BMGs using the injection method. Hence the large errors for these BMGs may have been caused by the unsatisfactory repeatability in sample preparation.

1. Correlation between ($T_{g\text{-}end} - T_{\alpha\text{-}p}$) and GFA

The DSC and $\alpha_L(T)$ traces of the Cu-, Zr-, Ti-, and Fe-based BMGs shown in Figs. 5(e1)-5(l1) display a similar shape in the crystallization region because of the simultaneous energy release and volume shrinkage caused by the atomic rearrangement from disorder to order during crystallization. For the Pd- and Mg-based BMGs shown in Figs. 5(a1)-5(d1), the sample length shrinkage exceeds the DIL instrument measurement range of 250 μm because of their low degree of strength in the large super-cooled liquid region.[1] The complete crystallization process cannot be observed in the $\alpha_L(T)$ traces, and the DSC and $\alpha_L(T)$ traces in Figs. 5(a1)-5(d1) thus do not look consistent. Figs. 5(a2)-5(i2) show that every composition has a peak in the $\alpha_L(T)$ traces, which is the interaction between the free volume generation during the glass transition process and sample softening above $T_{\alpha\text{-}p}$ under compressive stress. The relationship between $T_{\alpha\text{-}p}$ and $T_{g\text{-}end}$ for each of the 12 BMGs is plotted

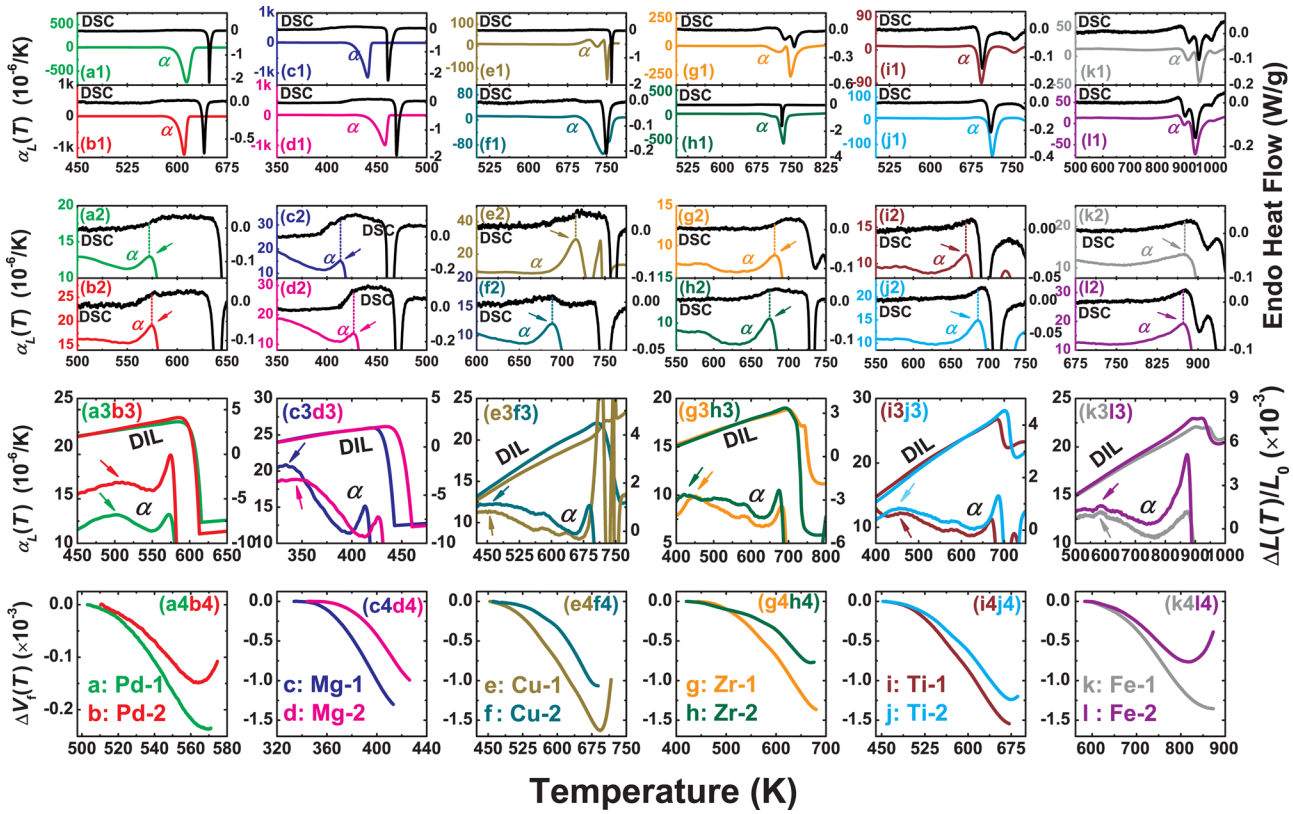

FIG. 5. [(a1)-(l1)] DSC and the $\alpha_L(T)$ traces of 12 Pd-, Mg-, Cu-, Zr-, Ti-, and Fe-based BMGs; [(a2)-(l2)] enlarged regions around the glass transition location, with the arrows indicating the $T_{\alpha\text{-}p}$; [(a3b3)-(k3l3)] DIL and $\alpha_L(T)$ traces, with the arrows indicating the $T_{sr\text{-}on}$ (the hypothesized $\alpha_L(T)$ traces and hypothesized DIL traces are not plotted for a clearer display; [(a4b4)-(k4l4)] Corresponding $\Delta V_f(T)$ curves. The sample diameters and heating rates of DSC and DIL were 2.0 mm and 5 K/min, respectively.

TABLE II. Summary of the thermal analyses by DSC ($T_{rg} = T_g/T_l$, $\gamma = T_x/(T_g + T_l)$, $\gamma_m = (2T_x - T_g)/T_l$, $\gamma_c = (3T_x - 2T_g)/T_l$), $\Delta V_{\text{f-sr}}$ and D_c of the 12 BMGs. The diameter of the samples was 2 mm. The heating rates in the DSC and DIL tests were 20 K/min and 5 K/min, respectively. The relative change is calculated as $(X_{\text{LargerGFA}} - X_{\text{SmallerGFA}})/X_{\text{SmallerGFA}}$, where X denotes T_{rg}, γ, γ_{m}, γ_{c}, and $\Delta V_{\text{f-sr}}$.

											Relative change (%) of				
Alloys	Composition	T_g (k)	T_x (k)	T_l (k)	T_{rg}	γ	γ_m	γ_c	$\Delta V_{\text{f-sr}} \times 10^{-3}$	D_c (mm)	Ref.	T_{rg}	γ	γ_m	γ_c	$\Delta V_{\text{f-sr}}$
a: Pd-1	$Pd_{40}Ni_{40}P_{20}$	576	671	991	0.595	0.424	0.759	0.841	0.237	25	29	16.0	9.4	15.9	15.8	−37.1
b: Pd-2	$Pd_{40}Cu_{30}Ni_{10}P_{20}$	577	656	836	0.690	0.464	0.879	0.974	0.150	72	30					
c: Mg-1	$Mg_{65}Cu_{25}Gd_{10}$	408	478	755	0.540	0.411	0.726	0.819	1.300	8	31	5.2	1.7	2.5	1.6	–23.5
d: Mg-2	$Mg_{58.5}Cu_{30}Dy_{11.5}$	433	500	762	0.568	0.418	0.744	0.832	0.994	12	32					
e: Cu-1	$Cu_{46}Zr_{47}Al_7$	705	781	1163	0.606	0.418	0.737	0.802	1.628	3	33	−0.4	3.4	6.3	8.9	−29.1
f: Cu-2	$Cu_{46}Zr_{42}Al_7Y_5$	672	772	1113	0.604	0.432	0.783	0.873	1.154	10	33					
g: Zr-1	$Zr_{58}Nb_3Cu_{16}Ni_{13}Al_{10}$	667	759	1160	0.575	0.415	0.734	0.813	1.365	7	34	−1.4	0	−0.3	0.2	−43.4
h: Zr-2	$(Zr-1)_{98.5}Y_{1.5}$	661	757	1165	0.567	0.415	0.732	0.815	0.773	14	34					
i: Ti-1	$Ti_{42.5}Zr_{2.5}Hf_5Cu_{42.5}Ni_{7.5}$	677	726	1203	0.563	0.386	0.644	0.685	1.545	2	35	0.8	0.6	1.0	1.1	−19.7
j: Ti-2	$Ti_{41.5}Zr_{2.5}Hf_5Cu4_{2.5}Ni_{7.5}Si_1$	680	730	1199	0.567	0.389	0.651	0.692	1.240	5	35					
k: Fe-1	$Fe_{48}Er_2Cr_{10}Mo_{19}C_{15}B_6$	840	895	1557	0.540	0.373	0.610	0.645	1.355	4	37	3.1	1.7	2.4	2.2	−43.6
l: Fe-2	$Fe_{48}Er_2Cr_{15}Mo_{14}C_{15}B_6$	843	895	1515	0.556	0.380	0.625	0.659	0.765	12	37					

separately in Fig. 6. It is clear that $T_{\alpha\text{-p}}$ is lower than $T_{\text{g-end}}$ for the 2.0 mm-diameter samples. Hence, the DIL method is unable to determine the entire free volume generation in the glass transition process. One interesting finding is that the $(T_{\text{g-end}} - T_{\alpha\text{-p}})$ of the composition with a larger GFA (D_c is given in Table II) is smaller than that with the same base metal but a smaller GFA. The implication is that, for BMGs of the same base metal, the viscosity of composition with a larger GFA decreases more slowly in the glass transition process, and $T_{\alpha\text{-p}}$ is thus closer to $T_{\text{g-end}}$ under the same compressive stress.

2. Sensitive correlation between $\Delta V_{\text{f-sr}}$ and GFA

As shown in Figs. 5(a3b3)-5(k3l3), all of the samples have a clear $T_{\text{sr-on}}$ above which the $\alpha_L(T)$ decreases continuously. $\Delta V_{\text{f}}(T)$ curves obtained using Eq. (3) are shown in Figs. 5(a4b4)-5(k4l4). It is clear that the compositions with a larger GFA display a smaller free volume release during structural relaxation than those with the same base metal but a smaller GFA. Table II lists several of the parameters related to GFA: the reduced glass transition temperature T_{rg}, which Turnbull[52] proposed as the first quantitative criterion

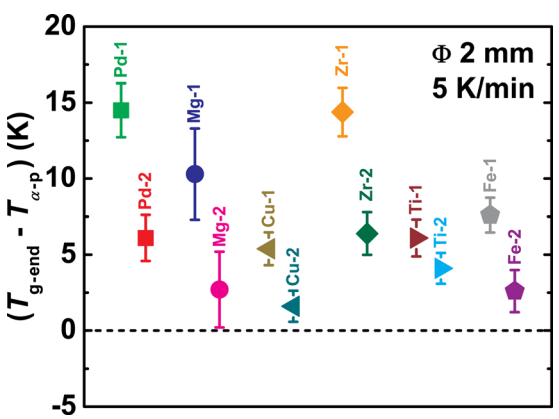

FIG. 6. Correlation between $T_{\alpha\text{-p}}$ and $T_{\text{g-end}}$ of the 12 BMGs.

for glass formation, a series of GFA indicators, γ, γ_{m}, and γ_{c}, developed from T_{rg}, as proposed by Liu *et al.*,[53–56] and the $\Delta V_{\text{f-sr}}$ quantified from the $\Delta V_{\text{f}}(T)$ curves in Figs. 5(a4b4)-5(k4l4). To allow quantitative comparison of the sensitivity of these parameters in terms of their ability to reflect a variation in GFA, their relative changes in each pair of BMGs with the same base metal are also listed. Table II shows that $\Delta V_{\text{f-sr}}$ is much more sensitive than the other criteria. The addition of a large amount of Cu to Pd-(Cu)-Ni-P (Ref. 30) leads to a remarkable decrease in T_{l}, and consequently increases T_{rg}, γ, γ_{m}, and γ_{c} by about 10%, although $\Delta V_{\text{f-sr}}$ changes even more dramatically, by about −40%. In addition, in the cases of a minor addition of Y to Cu-Zr-Al-(Y),[33] a similar composition but different rare earth elements for Mg-Cu-(Gd, Dy)[31,32] and a small variation in Cr and Mo for Fe-Er-(Cr, Mo)-C-B,[37] there is a significant increase in GFA, but the increase in T_{rg} and its derivatives is not very significant. However, there is still a quite obvious decrease in $\Delta V_{\text{f-sr}}$. Furthermore, for $(Zr_{58}Nb_3Cu_{16}Ni_{13}Al_{10})_{98.5}Y_{1.5}$ (Ref. 34) and $Ti_{42.5}Zr_{2.5}Hf_5Cu_{42.5}Ni_{7.5}$ (Ref. 35), which has the greatest GFA among the Ti-based BMGs without the addition of toxic beryllium and precious palladium, the addition of minor amounts of Y and Si changes T_{g}, T_{x}, and T_{l} only slightly. T_{rg} and its derivatives thus undergo a subtle change. GFA enhancement in these two compositions is deemed by their developers to be attributable to the change in their local atomic structure,[34,35] which is well supported by the obvious decreases in $\Delta V_{\text{f-sr}}$.

As discussed in Sec. III C, under the same sample diameter and heating rate, the $\Delta V_{\text{f-sr}}$ released during structural relaxation is determined primarily by the initial V_{f0} that is frozen from the free volume contained in the liquid metal. How much of the initial V_{f0} is contained in the amorphous solid depends on the amount of free volume in the liquid metal and how fast that free volume is annihilated with a change in temperature in the fast cooling process. These two factors are related to the viscosity[50] and fragility[48] of glass-forming liquid, respectively. Glass-forming liquid with a

higher viscosity and less fragility is more stable. In fast cooling, the lower atomic mobility of this kind of liquid results in greater difficulty in crystallization and therefore the enhancement of glass formation.[2,48,50–56] For this kind of liquid, the smaller initial V_{f0} is frozen into the amorphous solid after fast cooling. During the constant heating in the DIL test, a smaller $\Delta V_{f\text{-}sr}$ is thus released in the structural relaxation process. From the perspective of glass formation, $\Delta V_{f\text{-}sr}$ reflects the BMG structural feature inherited from the liquid metal, and T_{rg} and its derivatives are related primarily to the thermodynamic features. Compared to thermodynamic features, structural feature are more sensitive to the enhancement of GFA in BMGs with the same base metal.[51]

3. Close correlation between $\Delta V_{f\text{-}sr}$ and GFA

To investigate the effect of $\Delta V_{f\text{-}sr}$ on GFA for the BMGs with different base metals, the correlation between $\Delta V_{f\text{-}sr}$ and D_c^2 was also investigated. As shown in Fig. 7, there is a good linear relationship between $\Delta V_{f\text{-}sr}$ and Log D_c^2. In addition, $\Delta V_{f\text{-}sr}$ and Log D_c also have a linear relationship with the same accuracy ($R = 0.936$). $\Delta V_{f\text{-}sr}$ thus exhibits a close correlation with the GFA of these 12 BMGs. Furthermore, the regularity in Fig. 7 is similar to that of our previous results, and can be compared with the regularity obtained by Park *et al.*,[51] as discussed in our previous work.[1]

E. Comparison with other methods

Although our definition of $\Delta V_{f\text{-}sr}$ differs from that of the free volume change in other research,[7–11,13,16,17] the results of this research are still comparable to the free volume changes measured with the DSC, room temperature density, and positron annihilation lifetime methods. According to free volume theory,[7] the reduced free volume x can be expressed as $x = v_f/\gamma v^*$, where v_f is the free volume per atom volume and γv^* is a constant of order 0.1. The definite value of γv^* for most BMGs is lacking in the available literature. Hence, for convenience of discussion, γv^* is assumed to be 0.1 in the following comparison.

Based on the specific heat capacity data, Beukel and Sietsma[7] reported the Δx released in structural relaxation for as-quenched $Pd_{40}Ni_{40}P_{20}$ to be 0.96×10^{-2} (see Fig. 3 in Ref. 7), corresponding to a ΔV_f of 0.96×10^{-3}, which is obviously larger than our result of 0.237×10^{-3}. This inconsistency can be attributed to the ribbon sample used in Ref. 7. Using room temperature density data, Haruyama *et al.*[16,17] reported that the $\Delta\rho/\rho_0$ decreases in the isothermal annealing of $Pd_{40}Ni_{40}P_{20}$ BMG at 573 K for 2-12 min and $Pd_{42.5}Cu_{30}Ni_{7.5}P_{20}$ BMG at 549 K for 1-10 min are $0.10\text{-}0.53 \times 10^{-3}$ (see Fig. 5 in Ref. 16) and $0.06\text{-}0.5 \times 10^{-3}$ (see Fig. 4 in Ref. 16 and Fig. 4 in Ref. 17), respectively. In a study employing positron annihilation lifetime data, Wang *et al.*[13] reported the Δx released in the isothermal annealing of $Pd_{40}Cu_{30}Ni_{10}P_{20}$ BMG at 523 K for 2-16 h to be $0.3\text{-}0.5 \times 10^{-2}$ (see Fig. 4 in Ref. 13), which corresponds to a ΔV_f of $0.3-0.5 \times 10^{-3}$. Our results show that after 5 K/min of constant heating, the $\Delta V_{f\text{-}sr}$ of $Pd_{40}Ni_{40}P_{20}$ BMG released from $T_{sr\text{-}on}$ (503.1 K) to $T_{sr\text{-}end}$ (569.7 K) for 13 min is 0.237×10^{-3}, as shown in Fig. 5(a4b4). Also, the $\Delta V_{f\text{-}sr}$ of $Pd_{40}Cu_{30}Ni_{10}P_{20}$ BMG released from $T_{sr\text{-}on}$ (510.4 K) to $T_{sr\text{-}end}$ (564.0 K) for 11 min is 0.150×10^{-3}, as shown in Fig. 5(a4b4) and Fig. 2 of Ref. 1. Most of the values of these Pd-based BMGs with a very large GFA are less than 0.5×10^{-3} and comparable, in spite of the different sample fabrication conditions and heating processes used during measurement. In addition, for $Zr_{44}Ti_{11}Ni_{10}Cu_{10}Be_{25}$ (Vitreloy 1 b) BMG, which also has a very large GFA, in a study using enthalpy data, Busch *et al.*[9,10] reported the ΔV_f between the as-cast and equilibrium liquid to be only $0.3-0.5 \times 10^{-3}$ (see Fig. 13 in Ref. 9 and Fig. 4 in Ref. 10). These small values are comparable to the Pd-based BMGs. Furthermore, on the basis of DSC data, Zhang and Hahn[11] reported that the ΔV_f of $Zr_{45.0}Cu_{39.3}Al_{7.0}Ag_{8.7}$ BMG released in structural relaxation was 0.8×10^{-3} (see Figs. 10 and 11 in Ref. 11). Finally, using room temperature density and enthalpy data, Slipenyuk and Eckert[8] reported the ΔV_f of $Zr_{55}Cu_{30}Al_{10}Ni_5$ BMG to be $0.86\text{-}0.95 \times 10^{-3}$ after heating from room temperature to 675 K ($T_{g\text{-}on} = 695$ K) at 20 K/min and then subsequently cooling to room temperature at 100 K/min (see Figs. 5 and 6 in Ref. 8). As shown in Figs. 5(g2h2)-5(g4h4), for the $Zr_{58}Nb_3Cu_{16}Ni_{13}Al_{10}$ and $(Zr_{58}Nb_3Cu_{16}Ni_{13}Al_{10})_{98.5}Y_{1.5}$ BMGs, $T_{sr\text{-}end}$ was 15-25 K below $T_{g\text{-}on}$ and the $\Delta V_{f\text{-}sr}$ was 1.365×10^{-3} and 0.773×10^{-3}, respectively. The data of these four Zr-based BMGs, which have a smaller GFA than the Pd-based BMG and Vitreloy 1 b, are close to or larger than 0.8×10^{-3} and can be compared with each other, in spite of their different compositions, sample fabrication conditions and measurement heating processes.

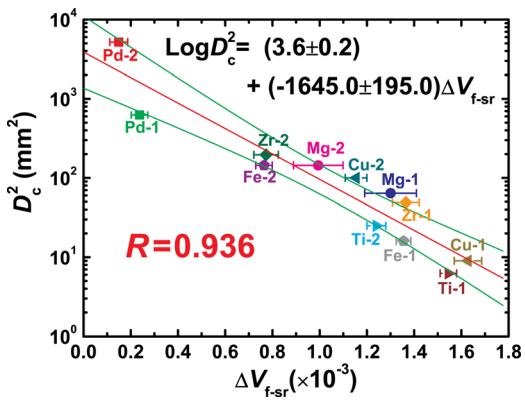

FIG. 7. Correlation between the GFA (D_c^2) and $\Delta V_{f\text{-}sr}$ of the twelve BMGs. The 95% confidence bands are also shown.

No comparisons of the Mg-, Cu-, Ti- and Fe-based BMGs were conducted because there are few available reports on the free volume measurements of these BMGs, although the aforementioned comparisons of the Pd- and Zr-based BMGs demonstrate the validity of the first characteristic free volume change $\Delta V_{f\text{-}sr}$. Unfortunately, this research was unable to measure the free volume generation during the entire glass transition process, i.e., the second characteristic free volume change $\Delta V_{f\text{-}gt}$ presented in Fig. 1(b), because of sample softening above $T_{\alpha\text{-}p}$ in the DIL test. The thermal expansion in the glass transition process and subsequent super-cooled liquid region could be measured without the sample softening effect using the synchrotron radiation XRD method[18–21] or a non-contact DIL instrument.[41] The clear

$T_{sr\text{-}on}$ below and above which there is an obvious linear and deviating thermal expansion, respectively, can be found for various compositions.[18–21,41] Hence, if the hypothesized thermal expansion rather than the relaxed sample thermal expansion is taken as the reference, then it is hoped that $\Delta V_{f\text{-}gt}$ and the subsequent free volume generation with a constant rate in the super-cooled liquid region shown in Fig. 1(b) can be quantified accurately using a non-contact DIL instrument.

IV. CONCLUSIONS

The free volume change $\Delta V_f(T)$ relative to a hypothesized amorphous reference state was measured using the DIL method. A characteristic free volume change, i.e., the free volume released in structural relaxation $\Delta V_{f\text{-}sr}$, was obtained on the basis of the $\Delta V_f(T)$ curve. The sample diameter and heating rate were found to have clear effects on $\Delta V_{f\text{-}sr}$. For the $Fe_{41}Co_7Cr_{15}Mo_{14}C_{15}B_6Y_2$ BMG, $\Delta V_{f\text{-}sr}$ increased with decreases in the sample diameter and heating rate. $\Delta V_{f\text{-}sr}$ measured by the DIL method under the same sample diameter and heating rate conditions allows convenient comparison among different BMGs. The comparison showed the GFA enhancement for Pd-, Mg-, Cu-, Zr-, Ti-, Fe-based BMGs to be sensitive to decreases in $\Delta V_{f\text{-}sr}$ and $(T_{g\text{-}end} - T_{\alpha\text{-}p})$. In addition, a good linear relationship between the $\Delta V_{f\text{-}sr}$ and Log D_c^2 or Log D_c of the 12 BMGs was found. It can therefore be concluded that $\Delta V_{f\text{-}sr}$ is sensitive to and closely correlated with GFA. Furthermore, the $\Delta V_{f\text{-}sr}$ measurement results for the Pd- and Zr-based BMGs are in good agreement with the free volume change measured with the DSC, room temperature density and positron annihilation lifetime methods. Finally, another characteristic free volume change, i.e., the free volume generated in the glass transition process $\Delta V_{f\text{-}gt}$, could not be quantified accurately in this research because of the sample softening effect. However, the $\Delta V_{f\text{-}gt}$ shows promise for measurements with other non-contact DIL instruments using the hypothesized amorphous reference state proposed herein.

It is very difficult to measure the absolute free volume of BMGs. Hence, it is feasible to adopt the characteristic free volume change to explore the relationship between the structure and properties of BMGs. In this exploration, $\Delta V_{f\text{-}sr}$, which is measured using the DIL method and reflects the structural features of amorphous solids, can play an important role given its comparability and convenience.

ACKNOWLEDGMENTS

This work is funded by the Science and Technology foundation of ShenZhen China (CXB200903090012A) and Two Hundred Plan for Talent Station of Shenzhen (Shenfu[2008] No.182).

[1]Q. Hu, X.-R. Zeng, and M. W. Fu, J. Appl. Phys. **109**, 053520 (2011).
[2]Y. Li, Q. Guo, J. A. Kalb, and C. V. Thompson, Science **322**, 1816 (2008).
[3]J. Tan, Y. Zhang, B. A. Sun, M. Stoica, C. J. Li, K. K. Song, U. Kuhn, F. S. Pan, and J. Eckert, Appl. Phys. Lett. **98**, 151906 (2011).
[4]J. C. Ye, J. Lu, C. T. Liu, Q. Wang, and Y. Yang, Nature Mater. **9**, 619 (2010).
[5]Q. Hu, X.-R. Zeng, and M.-W. Fu, Appl. Phys. Lett. **97**, 221907 (2010).
[6]Y. Q. Cheng and E. Ma, Appl. Phys. Lett. **93**, 051910 (2008).
[7]A. van den Beukel and J. Sietsma, Acta Metall. Mater. **38**, 383 (1990).
[8]A. Slipenyuk and J. Eckert, Scripta Mater. **50**, 39 (2004).
[9]Z. Evenson and R. Busch, Acta Mater. **59**, 4404 (2011).
[10]M. E. Launey, J. J. Kruzic, C. Li, and R. Busch, Appl. Phys. Lett. **91**, 051913 (2007).
[11]Y. Zhang and H. Hahn, J. Alloys Compd. **488**, 65 (2009).
[12]F. Ye, W. Sprengel, R. K. Wunderlich, H. J. Fecht, and H. E. Schaefer, Proc. Natl. Acad. Sci. U.S.A. **104**, 12962 (2007).
[13]J. F. Wang, L. Liu, J. Z. Xiao, T. Zhang, B. Y. Wang, C. L. Zhou, and W. Long, J. Phys. D: Appl. Phys. **38**, 946 (2005).
[14]K. M. Flores, D. Suh, R. H. Dauskardt, P. Asoka-Kumar, P. A. Sterne, and R. H. Howell, J. Mater. Res. **17**, 1153 (2002).
[15]C. Nagel, K. Ratzke, E. Schmidtke, J. Wolff, U. Geyer, and F. Faupel, Phys. Rev. B **57**, 10224 (1998).
[16]O. Haruyama, Intermetallics **15**, 659 (2007).
[17]O. Haruyama, H. Sakagami, N. Nishiyama, and A. Inoue, Mater. Sci. Eng., A **449-451**, 497 (2007).
[18]K. Hajlaoui, T. Benameur, G. Vaughan, and A. R. Yavari, Scr. Mater. **51**, 843 (2004).
[19]A. R. Yavari, A. Le Moulec, A. Inoue, N. Nishiyama, N. Lupu, E. Matsubara, W. J. Botta, G. Vaughan, M. Di Michiel, and A. Kvick, Acta Mater. **53**, 1611 (2005).
[20]D. V. Louzguine-Luzgin, A. R. Yavari, M. Fukuhara, K. Ota, G. Xie, G. Vaughan, and A. Inoue, J. Alloys Compd. **431**, 136 (2007).
[21]E. Pineda, I. Hidalgo, P. Bruna, T. Pradell, A. Labrador, and D. Crespo, J. Alloys Compd. **483**, 578 (2009).
[22]M. H. Cohen and D. Turnbull, J. Chem. Phys. **31**, 1164 (1959).
[23]D. Turnbull and M. H. Cohen, J. Chem. Phys. **34**, 120 (1961).
[24]D. Turnbull and M. H. Cohen, J. Chem. Phys. **52**, 3038 (1970).
[25]M. H. Cohen and G. S. Grest, Phys. Rev. B **20**, 1077 (1979).
[26]H. S. Chen, J. Appl. Phys. **49**, 3289 (1978).
[27]X. H. Chen, Y. Zhang, G. L. Chen, X. C. Zhang, and L. Liu, J. Appl. Phys. **103**, 113506 (2008).
[28]H. Kato, H. S. Chen, and A. Inoue, Scr. Mater. **58**, 1106 (2008).
[29]Y. He, R. B. Schwarz, and J. I. Archuleta, Appl. Phys. Lett. **69**, 1861 (1996).
[30]A. Inoue, N. Nishiyama, and H. Kimura, Mater. Trans., JIM **38**, 179 (1997).
[31]H. Men and D. H. Kim, J. Mater. Res. **18**, 1502 (2003).
[32]L. Zhao, H. Jia, S. Xie, X. Zeng, T. Zhang, and C. Ma, J. Alloys Compd. **504**, S219 (2010).
[33]D. H. Xu, G. Duan, and W. L. Johnson, Phys. Rev. Lett. **92**, 245504 (2004).
[34]X. Zhao, C. Ma, S. Pang, and T. Zhang, Philos. Mag. Lett. **89**, 11 (2009).
[35]C. Ma, H. Soejima, S. Ishihara, K. Amiya, N. Nishiyama, and A. Inoue, Mater. Trans. **45**, 3223 (2004).
[36]J. Shen, Q. J. Chen, J. F. Sun, H. B. Fan, and G. Wang, Appl. Phys. Lett. **86**, 151907 (2005).
[37]V. Ponnambalam, S. J. Poon, and G. J. Shiflet, J. Mater. Res. **19**, 1320 (2004). See here for information about the technique of NETZSCH DIL 402 C.
[38]http://www.netzsch-thermal-analysis.com/en/products/detail/pid,16.html (2011).
[39]A. Van Den Beukel and S. Radelaar, Acta Metall. **31**, 419 (1983).
[40]T. Zumkley, V. Naundorf, M. P. Macht, and G. Frohberg, Scr. Mater. **45**, 471 (2001).
[41]I. R. Lu, G. P. Gorler, H. J. Fecht, and R. Willnecker, J. Non-Cryst. Solids **274**, 294 (2000).
[42]Y. J. Huang, J. Shen, and J. F. Sun, Appl. Phys. Lett. **90**, 081919 (2007).
[43]X. H. Lin and W. L. Johnson, J. Appl. Phys. **78**, 6514 (1995).
[44]P. G. Debenedetti and F. H. Stillinger, Nature **410**, 259 (2001).
[45]P. Tuinstra, P. A. Duine, J. Sietsma, and A. Vandenbeukel, Acta Metall. Mater. **43**, 2815 (1995).
[46]W. L. Johnson, G. Kaltenboeck, M. D. Demetriou, J. P. Schramm, X. Liu, K. Samwer, C. P. Kim, and D. C. Hofmann, Science **332**, 828 (2011).
[47]J. Schroers, Adv. Mater. **22**, 1566 (2010).
[48]E. S. Park, J. H. Na, and D. H. Kim, Appl. Phys. Lett. **91**, 031907 (2007).
[49]R. Busch, J. Schroers, and W. H. Wang, MRS Bull. **32**, 620 (2007).
[50]S. Mukherjee, J. Schroers, Z. Zhou, W. L. Johnson, and W. K. Rhim, Acta Mater. **52**, 3689 (2004).
[51]E. S. Park and D. H. Kim, Appl. Phys. Lett. **92**, 091915 (2008).
[52]D. Turnbull, Contemp. Phys. **10**, 473 (1969).
[53]Z. P. Lu and C. T. Liu, Acta Mater. **50**, 3501 (2002).
[54]Z. P. Lu and C. T. Liu, Phys. Rev. Lett. **91**, 115505 (2003).
[55]X. H. Du, J. C. Huang, C. T. Liu, and Z. P. Lu, J. Appl. Phys. **101**, 086108 (2007).
[56]S. Guo and C. T. Liu, Intermetallics **18**, 2065 (2010).